Low-temperature silver sintering by colloidal approach

Maxime Bronchy, Jean-Charles Souriau, Jean-Marc Heintz, Céline Feautrier, David Henry, Etienne Duguet, Laurent Mendizabal, Gilles Simon, Mona Tréguer-Delapierre

Low-temperature silver sintering by colloidal approach

Maxime Bronchy
ICMCB UMR 5026
Univ. Bordeaux, CNRS, Bordeaux INP
33600 Pessac, France
Univ. Grenoble Alpes, CEA, LETI
38000 Grenoble, France
maxime.bronchy@icmcb.cnrs.fr

Céline Feautrier
Univ. Grenoble Alpes, CEA, LETI
38000 Grenoble, France
celine.feautrier@cea.fr

Laurent Mendizabal
Univ. Grenoble Alpes, CEA, LETI
38000 Grenoble, France
laurent.mendizabal@cea.fr

Jean-Charles Souriau
Univ. Grenoble Alpes, CEA, LETI
38000 Grenoble, France jean-charles.souriau@cea.fr

David Henry
Univ. Grenoble Alpes, CEA, LETI
38000 Grenoble, France
david.henry@cea.fr

Gilles Simon
Univ. Grenoble Alpes, CEA, LETI
38000 Grenoble, France
gilles.simon@cea.fr

Jean-Marc Heintz
ICMCB UMR 5026
Univ. Bordeaux, CNRS, Bordeaux INP
33600 Pessac, France
0000-0002-1082-5714

Etienne Duguet
ICMCB UMR 5026
Univ. Bordeaux, CNRS, Bordeaux INP
33600 Pessac, France
0000-0002-0675-5987

Mona Treguer-Delapierre
ICMCB UMR 5026
Univ. Bordeaux, CNRS, Bordeaux INP
33600 Pessac, France
mona.treguer@icmcb.cnrs.fr

***Abstract*— The interest of silver nanostructures has surged in recent years as they are becoming promising materials in a growing number of applications. In particular, they have received intense attention for their use as lead-free die attach materials, photoactive devices engineering or more broadly electronic packaging. One of the challenges is the elaboration of conductive and printable patterns by Low-Temperature and Pressureless Sintering Techniques (LTPST) to achieve electric circuits on heat-sensitive substrates such as paper, plastic, polymeric substrates. Here, we present a facile method for synthesizing conductive patterns at low temperature based on the formation of self-assembled Ag nanocubes on Active Metal Brazing (AMB) substrates. The elaboration of 3-D arrays with nanogap of 2-3 nm between the cubic building units allows to get dense and compact packed nanoparticle solids which sinter at lower temperature than conventional commercial silver pastes. The impact of the capping agent and the size of the building units on the sintering properties were investigated and discussed.**

Keywords — Silver, sintering, nanocubes, LTPST, self-assembly, supercrystals

I. INTRODUCTION

Silver-based sintering is currently considered as a promising die attach material technique as an alternative to brazing. Silver is an excellent compromise in terms of cost, processability, electrical and thermal conductivity. Several studies demonstrated the feasibility and high electrical, thermal and mechanical performances of die attach based on sintered silver. It allows to proceed to sinter at lower temperature (LT) compared to lead or gold based solders [1-4]. Further, the recent development of pressureless silver sintering techniques is a crucial breakthrough providing to extent the application area to mechanically sensible assemblies. There are currently several industrial groups which commercialize many silver-based sintering pastes. Such pastes typically include a solvent, an organic stabilizer and silver particles. The impacts of the nanocrystal size and surface chemistry on the sintering properties have been extensively studied [5, 6]. Nanosilver pastes can be sintered at lower temperature compared to bulk silver. However, the influence of the nanocrystal shape and of their potential self-assembly has largely been overlooked.

Here, we report a detailed study of how the self-assembly of superlattice of Ag nanocubes prior the sintering affects the densification of the nanocrystals upon a heating treatment. The cubic morphology of the nanocrystals was chosen because the cubic shape of superlattice is the most compact structure possible with building units (100 % vs. 74 % for close-packed isometric spheres [7]).

A. Nanosilver pastes and pressureless sintering

The current Low-Temperature and Pressureless Sintering Techniques (LTPST) based on silver have drawn increasing attention in the last decade because of their high performances and ease of use. These technologies offer the advantage of forming dense interconnections without application of uniaxial pressure and presenting properties close to those of pressure sintering techniques for die attach applications. These pressureless sintering formulations are mainly hybrid pastes made of mixtures of micrometric and nanometric size Ag particles, for a total silver quantity higher than 90 wt%, the rest of the composition including solvents, organic stabilizers and additives. The high densification level is obtained, despite the lack of uniaxial pressure, thanks to the incorporation of nanometric size particles, well known to be more reactive, and to enhance densification. The phenomenon is explained by the melting-point depression model, which predicts the melting temperature reduction with the size of the spherical metal nanoparticles, experimentally demonstrated on Au nanoparticles by Ph. Buffat and J-P. Borel [8] and simulated on Ag nanoparticles by Luo et al. [9]. The melting-point depression may be approximated by equation (1):

$$T_m(D) = T_{m0}\,(1 - (\beta / D))\ [\mathrm{K}] \qquad (1)$$

T_m and T_{m0} (in K) representing the melting temperature of a spherical nanoparticle and the melting temperature of the corresponding bulk material, function of the particles diameter D (in nm) and β a constant (in nm) relative to the studied material. Applied to silver, the relationship shows a

sharp reduction of silver nanoparticles melting temperature below 20 nm, indicating the high thermal instability of small diameter nanoparticles. The tendency is equally observed in the case of an effective sintering temperature reduction when the particles diameter decreases. Transposed to sintering, this model allows to significantly reduce the sintering temperature using nanometer size particles to enhance sintering properties at LT. The strategy is particularly studied in the current development of nanosilver inks at room temperature [5, 6]. They have attracted considerable interest as one of the most promising Ag-based conductive materials.

B. *Morphology control and self-assembly*

Most of the studies on sintering processes of silver nanoparticles are usually based on spherical nanoparticles. Besides nanoparticles with spherical morphology, nanomaterials with other morphologies, *e.g.* flakes or plates, have been mixed in pastes. For example, Arakawa *et al.* have embedded micron-sized Ag flakes into the paste to favor a flat deposition of microparticles on the substrate during the paste printing [10]. This strategy improves the Ag density onto the substrate before sintering and is considered as one of the most efficient LT sintering process. On the other hand, Qun *et al.* have demonstrated that self-assembly of spherical nanoparticles prior to the sintering step also allows to lower the sintering temperature to about 200°C [11]. But the sintering mechanism of such approaches remains unknown. In this report, we explored a new approach depicted in the scheme of Figure 1. To achieve LT sintering of silver nanoparticles, we produced silver nanoparticles with a cubic morphology, self-assembled them into supercrystals on a solid substrate and finally proceeded to their sintering. High-quality silver nanocubes with uniform morphology and good size calibration were produced in high yield by colloidal approaches [12-14]. The NCs self-assemblies were made by a drop-casting method which consists of a slow evaporation of colloidal dispersion at controlled temperature [15-17]. Sintering tests on the superlattices was achieved on a precision heating plate under inert atmosphere.

II. EXPERIMENTS

A. *Materials*

Silver nitrate ($AgNO_3$, 99.99%w., Sigma-Aldrich), silver trifluoroacetate (CF_3COOAg, 99.99%w., Sigma-Aldrich), polyvinylpyrrolidone (PVP 10k, Mw ≈ 10 000, Sigma-Aldrich), cetyltrimethylammonium chloride (CTAC, 98%w., Sigma-Aldrich), ethylene glycol (EG, Baker analysed reagent, J.T.Baker), 1,2-propandiol (PG, 99%, Sigma-Aldrich), sodium borohydride ($NaBH_4$, 98%w., Sigma-Aldrich), sodium hydrosulfide hydrate ($NaSH•xH_2O$, Sigma-Aldrich), L-ascorbic acid ($C_6H_8O_6$, 98%w., Sigma-Aldrich), 1-octadecanethiol (99%w., Sigma-Aldrich), deionized water (DI water, 18.2MΩ) and absolute ethanol were used throughout the experiment without further purification.

B. *Ag nanocubes synthesis*

Large quantities of Ag NCs were synthesized with high yield by two approaches. First, we used a modified protocol from Zhang *et al.* in polyol medium [13]. This approach produces uniform cubes in high yield and in a single run. In a typical process, 60 mL of EG were introduced into a 250 mL round-bottom flask and pre-heated in an oil bath set to 150°C under magnetic stirring with a Teflon-coated stir bar. After 50 min, a flow argon (Ar) is introduced up to the solution at a flow rate of 500 mL/min. After 10 min of Ar protection, 0.7 mL of a 3 mM NaSH solution in EG is added, followed by 15 mL of a 20 mg/mL PVP10k solution in EG. After 8 min of homogenization, 5 mL of a 48 mg/mL $AgNO_3$ solution in EG were quickly injected in the reaction medium. The total volume of reaction medium was set to 80.07 mL. After 20 min of reaction, the particles growth was quenched by transferring the flask in an ice-bath. The obtained Ag NCs were washed once with acetone and twice with ethanol to remove polyol and PVP in excess via centrifugation (12,000g, 20 min). Finally, the Ag NCs were redispersed in a polyol. In such experimental conditions, the Ag NCs exhibit a mean length of 25 nm and are coated with PVP that avoids aggregation. Nanocubes of different length were also produced by increasing the reaction time. The second protocol was adapted from Lin *et al.* procedure and yielded to the formation of Ag NCs in aqueous medium [14]. A silver-seed solution was prepared in a 50 mL round-bottom flask immersed in an oil bath set to 30°C. 10 mL of 0.5 mL CTAC aqueous solution were introduced in the flask under magnetic stirring with a Teflon-coated stir bar. After 10 min, 25 µL of a 0.1 M freshly prepared $AgNO_3$ aqueous solution was introduced in the flask and left under stirring for 5 min. Next, 0.45 mL of a 0.08 M ice-cold $NaBH_4$ aqueous solution was quickly injected in the reaction medium. The flask was stirred for 1 h at 30°C to decompose excess of $NaBH_4$ by water. The as-prepared silver-seed solution was used in the Ag NCs growth protocol. In order to monitor the Ag NCs size, 43 and 39.5 mL of DI water and 40 mg of CTAC were added in two 100 mL round-bottom flasks, immersed in oil bath set to 60°C under magnetic stirring with a Teflon-coated stir bar. Each flask corresponds to 35 nm and 23 nm Ag NCs growth reactions, respectively. Next 1.5 and 5 mL of the silver-seed solution were introduced, respectively, followed by 500 µL of a 0.1 M CF_3COOAg aqueous solution in each flask. The reaction medium was then left under magnetic stirring at 60°C for 20 min. After homogenization, 5 mL of a 0.1 M L-AA aqueous solution was quickly added in each flask and the solutions were kept at 60°C under magnetic stirring for 90 min. After 90 min of reaction, the particles were washed three times with DI water

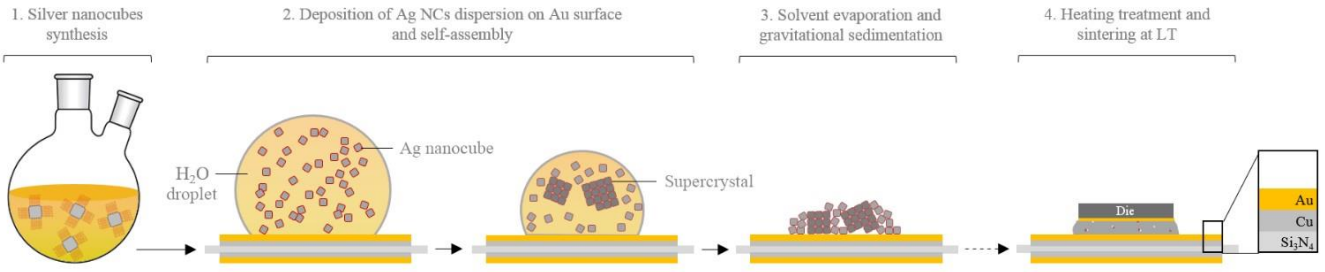

Fig. 1. Experimental strategy for the development of LT silver sintering technique by ordered supercrystals deposition on AMB substrate. Organic stabilizer protecting the Ag nanocubes from aggregation is reported in red.

by centrifugation (12 000 rpm, 20 min) and redispersed in 2 mL of DI water. Throughout the paper, the as-prepared dispersions are called Ag@PVP and Ag@CTAC dispersions, respectively.

C. Self-assembly by drop-casting

The Ag NCs dispersions (15 µL droplet concentration) were deposited on AMB substrates (Si_3N_4, Au metallization) previously treated by plasma cleaning. Some of the AMB surfaces being hydrophobic, they were functionalized to maximize the contact angle of deposited dispersion droplets. For this purpose, the AMB substrates were immersed in a 50 mL of 1 mM 1-octodecanethiol ethanolic solution for 24 h, and then dried at room temperature. The liquid of the NCs dispersion deposited on the AMB substrates was evaporated at 22°C in a closed environment (glass bell) until total solvent evaporation (≈ 3h). The as-prepared deposition was then stored under argon.

D. Pressureless sintering process

The samples were then annealed at different temperatures: 135, 150 or 185°C under Ar atmosphere with a flow rate of 500 mL/min to sinter the nanocubes. The rise in temperature and the plateau were set to 1 and 2 h, respectively. Supplementary long time sintering tests were carried out at lower temperature and longer dwell time (135°C, 16 h).

E. Instrumentation

The colloidal suspensions were analyzed by a Shimadzu UV-3600 UV-visible-near IR spectrometer. Transmission electron microscopy (TEM) was performed with a JEOL 1400F. Samples of AgNCs onto the substrates were imaged by Scanning Electron Microscopy (SEM) with a JEOL 6700 FEG (PLACAMAT facility), a JSM-IT500HR (CEA-LETI facility) or a FEI Helios 600i (R. Castaing facility). A mechanical polishing was performed with Struers tegramin-30 polisher using in sequence: SiC foil 1200, diamond pastes 9 µm, 3 µm and 1µm, following by colloidal 40-50 nm silica paste.

III. Results

A. Ag nanocrystals and superlattice formation.

Ag NCs with an edge length ranging from 20 to 60 nm were produced in polyol or aqueous medium. Polyol synthesis yielded nano-objects capped with a PVP layer that prevents coalescence and oxidation [10,11] (Fig. 2a). The PVP chains are known to be stable upon 150°C. The synthesis in aqueous medium yielded to the production of Ag NCs capped with CTAC (Fig. 2b). The CTAC molecules form a well-defined bi-layer onto the metal surface. The order within the bilayer is derived from the alkyl chain-chain interactions. Because of their very narrow size distribution (<10%), the nanocubes capped with CTAC self-organize into large and compact monolayers upon deposition on the carbon grid (Fig. 2b). The Ag NCs remain separated by the capping ligand layer coating each particle. UV-visible analyses were performed to confirm the sizes and morphologies of the as-synthetized Ag NCs. The normalized absorption peaks corresponding to Localized Surface Plasmon Resonances exhibit a red-shifting when the particles size increases; the second peak fits with secondary and coupling resonance modes. The Full Width at Half Maximum (FWHM) of the main peak, typically less than 50 nm, attests a narrow size distribution of the synthetized particles (Fig. 2c). Self-assembly protocol was carried out on different batches of Ag@CTAC onto a solid substrate. Fig. 3 shows the SEM images of well-defined cubic superlattices formed from Ag NCs of 32 ± 4 and 21 ± 3 nm within a couple of hours. Whatever their size, the cubes organized themselves spontaneously in 3D forming individual supercrystals that were mainly stacked in random positions or more rarely isolated on the substrate. Their typical lateral size is in the range of 0.5 – 3 µm (Table 1). Depending on the wetting properties of the substrate, the evaporation rate, and the concentration of the nanocrystals in the dispersion, supercrystals of different morphologies were obtained. Large-structureless superlattices were obtained under fast evaporation. Conversely, large 3D superlattices took place under slow evaporation. Generally, we observed on functionalized gold substrates the formation of supercrystals with a well-defined cubic shape onto very large distances (several micrometers) upon evaporation of the solvent for a couple of hours. The cubic arrangement revealed some stacking faults which are likely due either to local heterogeneity of the nanocubes shapes or to a local disruption of the growth process. The observed cubic shape is the most compact structure possible with cubic building units. Detailed analysis by SEM revealed that the relative compacity of the superlattice was between 0.7 and 0.8. The gap in between two building units was about 2-3 nm. This gap is filled by the ligand, *i.e.* the capping agent. Its nature was also investigated. Not surprisingly, the superlattices structure formed from Ag@PVP were less regular and some self-assemblies were amorphous.

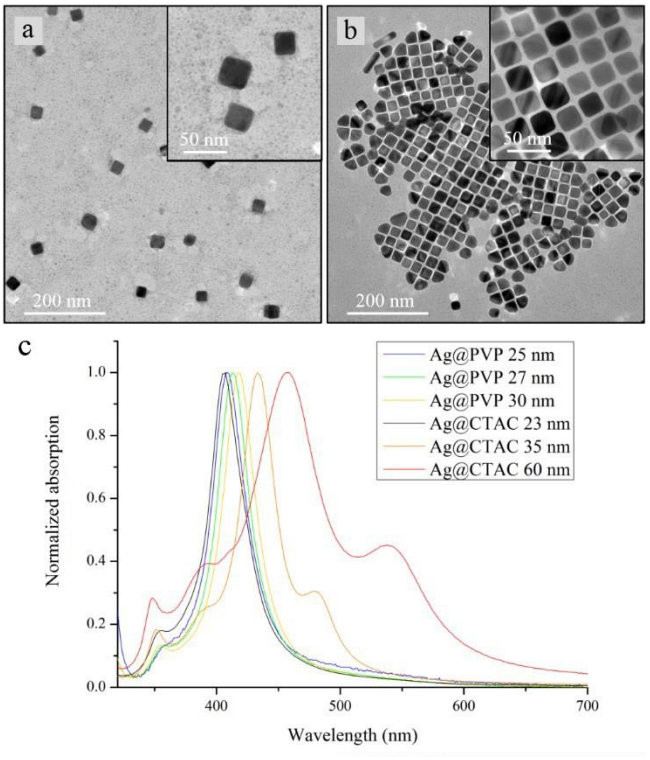

Fig. 2. TEM images of Ag NCs corresponding to Ag@PVP (a) and Ag@CTAC (b) dispersions, and UV-visible absorption spectra of Ag NCs prepared in polyol and aqueous medium (c).

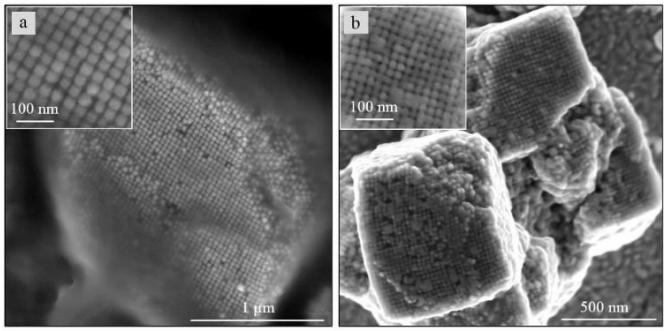

Fig. 3. SEM images of 32 ± 4 (a) and 21± 3 nm (b) Ag NCs supercrystals formed by drop-casting.

TABLE I. STURCTURAL PARAMETERS OF SUPERCRYSTALS

Ag NCs size (nm)*	32 ± 4	21 ± 3
Interdistance beetween NCs (nm)	3 ± 1	2 ± 1
Supercrystals size (µm)	0.8 to 3	0.5 to 2

B. Sintering results

For Ag@PVP samples prepared from Ag NCs of 27 nm and deposited on Au metallization layer, the sintering begun at 150°C. The Ag NCs lost their cubic morphology, forming sintered domains higher than 50 nm. At temperature close to 185°C, the sintered domains have clearly grown in size, being higher than 100 nm as shown in the top-view and cross-section images (Fig. 4). The section even shows sub-micrometric Ag grain through the full thickness of the sample and no delamination at the surface of the substrate was observed. The densification level may be differentiated in two domains (Fig. 4 bottom). The relative densities of the red and green domains were estimated to be 0.96 and 0.92, respectively. During heating, evaporation of solvent and segregation of the capping agent through the porosity also took place, even if some residual PVP quantity could be still trapped into the porosity. It resulted in the presence of an open porosity at the surface of the sintered Ag layer, as shown on the three samples. As a matter of fact, the observed high relative density and grain growth prove the occurrence of a very efficient sintering process of the Ag NCs. Thermogravimetric analysis (TGA) of the capping agents used, PVP or CTAC, under Ar atmosphere showed no observable transitions below 200°C aside from the evaporation of some residual solvent. This suggests that structural transformations of the Ag NCs are not directly influenced by the thermal behavior of the capping ligand.

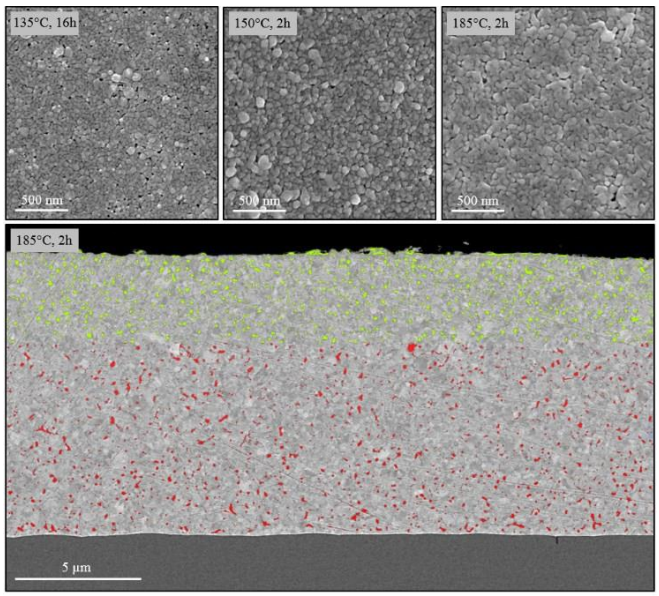

Fig. 4. SEM images of the silver sintered samples for 16 h at 135°C, 2 h at 150°C and 2 h at 185°C in top-view. The cross-sectional view correspond to the sintered sample for 2 h at 185°. Red and green domains indicate the residual porosity of the densification domains, corresponding respectively to 0.96 and 0.92 of relative density.

IV. SUMMARY AND OUTLOOK

The interest of 3-D superlattices formed by the self-assembly of monodisperse individual cubic silver nanocrystals yield to conductive materials that sinter at lower temperature than the commercial silver pastes. The preliminary sintering test, performed in open environment revealed promising results: no delamination and good densification levels upon 150°C. The sintering of the cubic silver nanoparticles was multidirectional. Further studies will investigate the effect of an order of the packing on the sintering properties and electrical/thermal performances. Such studies will be extended to other types of particles such as copper ones.

ACKNOWLEDGMENT

We acknowledge the Raymond Castaing team (UMS 3623, Toulouse) and Placamat team (UMS 3626, Pessac) for both sharing their electronic microscopy expertise. We also thank Mr Alain Gueugnot for the preparation and polishing of the sintered samples (CEA Leti).

REFERENCES

[1] M. Knoerr, S. Kraft and A. Schletz, "Reliability assessment of sintered nano-silver die attachment for power semiconductors", *2010 12th Electronics Packaging Technology Conference*, 2010.

[2] T. Wang, X. Chen, G. Lu and G. Lei, "Low-Temperature Sintering with Nano-Silver Paste in Die-Attached Interconnection", *Journal of Electronic Materials*, vol. 36, no. 10, pp. 1333-1340, 2007.

[3] K. Suganuma, S. Sakamoto, N. Kagami, D. Wakuda, K. Kim and M. Nogi, "Low-temperature low-pressure die attach with hybrid silver particle paste", *Microelectronics Reliability*, vol. 52, no. 2, pp. 375-380, 2012.

[4] H. Zhang, W. Li, Y. Gao, H. Zhang, J. Jiu and K. Suganuma, "Enhancing Low-Temperature and Pressureless Sintering of Micron Silver Paste Based on an Ether-Type Solvent", *Journal of Electronic Materials*, vol. 46, no. 8, pp. 5201-5208, 2017.

[5] D. Wakuda, K. Kim and K. Suganuma, "Room temperature sintering mechanism of Ag nanoparticle paste", *2nd Electronics Systemintegration Technology Conference*, 2008.

[6] S. Magdassi, M. Grouchko, O. Berezin and A. Kamyshny, "Triggering the Sintering of Silver Nanoparticles at Room Temperature", *ACS Nano*, vol. 4, no. 4, pp. 1943-1948, 2010.

[7] A. Gantapara, J. de Graaf, R. van Roij and M. Dijkstra, "Phase Diagram and Structural Diversity of a Family of Truncated Cubes: Degenerate Close-Packed Structures and Vacancy-Rich States", *Physical Review Letters*, vol. 111, no. 1, 2013.

[8] P. Buffat and J. Borel, "Size effect on the melting temperature of gold particles", *Physical Review A*, vol. 13, no. 6, pp. 2287-2298, 1976.

[9] W. Luo, W. Hu and S. Xiao, "Size Effect on the Thermodynamic Properties of Silver Nanoparticles", *The Journal of Physical Chemistry C*, vol. 112, no. 7, pp. 2359-2369, 2008.

[10] Kyocera, "Paste composition, semiconductor device, and electrical/electronic component", WO2019065221A1, 2018.

[11] Y. Huang, N. Wang, Y. Chen, Z. Lu and Q. Chen, "Silver Slurry containing multiple-hydrogen bon supermolecule self-assembly system, and application thereof", CN103606394B, 2020.

[12] Q. Zhang, W. Li, L. Wen, J. Chen and Y. Xia, "Facile Synthesis of Ag Nanocubes of 30 to 70 nm in Edge Length with CF3COOAg as a Precursor", *Chemistry - A European Journal*, vol. 16, no. 33, pp. 10234-10239, 2010.

[13] Q. Zhang, C. Cobley, L. Au, M. McKieran, A. Schwartz, L.-P. Wen, J. Chen and Y. Xia, "Production of Ag Nanocubes on a Scale of 0.1 g per Batch by Protecting the NaHS-Mediated Polyol Synthesis with Argon", *ACS Applied Materials & Interfaces*, vol. 1, no. 9, pp. 2044-2048, 2009.

[14] Z. Lin, Y. Tsao, M. Yang and M. Huang, "Seed-Mediated Growth of Silver Nanocubes in Aqueous Solution with Tunable Size and Their Conversion to Au Nanocages with Efficient Photothermal Property", *Chemistry - A European Journal*, vol. 22, no. 7, pp. 2326-2332, 2016.

[15] C. Liao, Y. Lin, K. Chanda, Y. Song and M. Huang, "Formation of Diverse Supercrystals from Self-Assembly of a Variety of Polyhedral Gold Nanocrystals", *Journal of the American Chemical Society*, vol. 135, no. 7, pp. 2684-2693, 2013.

[16] A. Guerrero-Martínez, J. Pérez-Juste, E. Carbó-Argibay, G. Tardajos and L. Liz-Marzán, "Gemini-Surfactant-Directed Self-Assembly of Monodisperse Gold Nanorods into Standing Superlattices", *Angewandte Chemie International Edition*, vol. 48, no. 50, pp. 9484-9488, 2009.

[17] J. Henzie, M. Grünwald, A. Widmer-Cooper, P. Geissler and P. Yang, "Self-assembly of uniform polyhedral silver nanocrystals into densest packings and exotic superlattices", *Nature Materials*, vol. 11, no. 2, pp. 131-137, 2011.